Roles of $G_{o\alpha}$ Tryptophans in GTP Hydrolysis, GDP Release, and Fluorescence Signals†

Keng-Li Lan,‡ Ann E. Remmers,‡ and Richard R. Neubig*,‡,§

Departments of Pharmacology and Internal Medicine/Hypertension, The University of Michigan, Ann Arbor, Michigan 48109-0632

Received August 26, 1997; Revised Manuscript Received October 8, 1997

ABSTRACT: Single tryptophan mutants of a histidine-tagged $G_{o\alpha}$ (W132F and W212F) were prepared to examine the functional and spectroscopic role of tryptophan in $G_{o\alpha}$. The mutants bound GTPγS with high affinity and showed only modest changes in GDP affinity. GTPγS-stimulated intrinsic fluorescence changes were completely abolished by removal of W^{212} but were not affected by elimination of W^{132}. In contrast, both W^{132} and W^{212} contributed to the fluorescence signal from binding of methylanthraniloyl-GTPγS (mGTPγS). W132F and W212F mutants showed 57% and 34% of the mGTPγS fluorescence change of wild type (WT), respectively. The decreased fluorescence signals were not due to reduced activation of the W212F protein by nucleotide as protection from tryptic digestion was unchanged. The kinetics of nucleotide binding and hydrolysis were also altered in both mutants. GDP dissociation was slower (0.14 min^{-1}) for W132F and faster (0.54 min^{-1}) for W212F than for WT (0.25 min^{-1}). As expected, the steady-state V_{max} for GTPase was lower for W132F, but surprisingly it was also lower for W212F despite faster GDP release. Single turnover kinetics revealed a lower k_{cat} for W212F (0.52 min^{-1}) compared to WT (1.39 min^{-1}) and W132F (1.0 min^{-1}). Thus, W^{212} in $G_{o\alpha}$ makes a dominant contribution to both intrinsic and extrinsic fluorescence signals upon α subunit activation. In addition, both tryptophans modulate the kinetics of nucleotide binding and hydrolysis.

Receptor-mediated activation of heterotrimeric GTP[1] binding proteins is a common mechanism for transducing biological signals. Cell surface receptors regulate G proteins by stimulating the release of GDP from the α subunit of the G protein, allowing GTP to bind and activate the G protein. G protein activation *in vitro* involves α subunit dissociation from $\beta\gamma$ subunits. The dissociated α and $\beta\gamma$ subunits interact with effector proteins to modulate cellular responses including second messenger metabolism and ion channel function (*2*−*5*). G protein deactivation is mediated by an intrinsic α subunit GTPase activity which can be enhanced by GTPase accelerating proteins (*6*−*8*), and upon deactivation, α and $\beta\gamma$ subunits reassociate. While much is known about G protein function, precise definition of G protein conformational changes during receptor-mediated activation and deactivation is incomplete.

The best understood G protein mechanism is the rhodopsin-mediated activation of transducin in the retinal rod outer segment. Conformations of rhodopsin are easily studied via the retinal chromophore. Changes in the transducin intrinsic fluorescence, due largely to W^{207} (*9*), have been used to monitor activation and deactivation (*10*, *11*) and to model the mechanism of the rhodopsin-stimulated activation−deactivation cycle of transducin (*12*). Kinetic mechanisms of the predominant G proteins purified from brain (G_o and G_i) have also been studied extensively in detergent solution and in phospholipid vesicles (*2*). G_o is the most abundant heterotrimeric G protein in mammalian brain. It contains two tryptophans in the α subunit. Upon activation by GTP and magnesium, the intrinsic fluorescence of $G_{o\alpha}$ tryptophan increases (*13*). The effects of $\beta\gamma$ subunits, ions, and activating ligands on $G_{o\alpha}$ tryptophan fluorescence have been well characterized (*14*, *13*). The X-ray structure of GDP- and GTPγS-liganded α_{i1} indicates major differences in the orientation of the α2 helix containing Trp 211 (*15*). In the GTPγS-bound state, the α2 helix is constrained with the Trp in a hydrophobic environment, which is presumably the cause of the tryptophan fluorescence increase. With GDP bound, this helix in transducin rotates (*16*, *15*), and in $G\alpha_{i1}$, it is disorganized and exposed to solvent (*17*, *18*).

One of our goals has been to study real time G protein activation and deactivation kinetics. We have previously reported that *N*-methyl-3′-*O*-anthraniloyl (MANT) guanine nucleotide analogs are useful environmentally sensitive fluorescent probes to study heterotrimeric G protein activation (*1*). A strong excitation peak was seen at 280 nm upon

† This work was supported by NIH Grant GM 39561.

* Address correspondence to this author at the Department of Pharmacology, 1301 MSRB III, 1150 W. Medical Center Dr., Ann Arbor, MI 48109-0632. Phone: 313 763-3650. FAX: 313 763-4450. E-mail: RNeubig@umich.edu.

‡ Department of Pharmacology.

§ Department of Internal Medicine/Hypertension.

[1] Abbreviations: DTT, dithiothreitol; G protein, GTP-binding protein; GDP, guanosine diphosphate; GTP, guanosine triphosphate; GTPγS, guanosine 5′-*O*-(3-thiotriphospate); Gpp(CH_2)p, guanylyl (β,γ-methylenediphosphate); Gpp(NH)p, guanylyl 5′-imidodiphosphate; HED-NML, 50 mM Hepes, pH 8.0, 1 mM EDTA, 1 mM DTT, 10 mM $MgSO_4$, 20 ppm deionized Lubrol; $His_6G_{o\alpha}$, hexa-histidine-tagged G_o protein α subunit; IPTG, isopropyl β-D-thiogalactopyranoside; MANT, *N*-methyl-3′-*O*-(3-thiotriphosphate); mGXP, MANT guanine nucleotide; $T_{50}\beta_{20}P_{0.1}$, 50 mM Tris-HCl, (pH 8.0), 20 mM 2-mercaptoethanol, and 0.1 mM phenylmethanesulfonyl fluoride.

S0006-2960(97)02122-3 CCC: $15.00
Published on Web 01/01/1998

binding of MANT derivatives of GTP to $G\alpha_o$ or $G\alpha_i$, which suggests that resonance energy transfer from G_α tryptophans to the MANT moiety was occurring (*1*). The magnitude of the fluorescence increase depended on the type of nucleotide. mGTPγS showed the greatest signal followed by mGppNHp, mGppCH_2p, and mGTP, while mGDP and mGDPβS gave very small signals (*19*). This rank order of MANT fluorescence signals correlated with the degree of G protein activation. Dissociation kinetics and trypsin protection data provided evidence for a conformational equilibrium between the active and inactive states, when the mGTP derivatives (especially mGppCH_2p) were bound (*19*).

To further understand the determinants of the MANT-guanine nucleotide fluorescence signals and to prove that energy transfer from tryptophan was occurring, we mutated the tryptophan residues in the $G_o\ \alpha$ subunit and studied their spectral and functional properties. As previously shown for W^{207} in transducin, tryptophan 212 in $G_{o\alpha}$ is essential for the intrinsic fluorescence signal. It contributes significantly to the extrinsic fluorescence signal from mGTPγS, but in this case, tryptophan 132 also plays a role. Both tryptophans influence nucleotide binding kinetics while mutation of W^{212} also significantly reduces the k_{cat} for GTP hydrolysis. Thus, the enhancement of fluorescence of mGTP derivatives on binding to $G_{o\alpha}$ does include a significant component of energy transfer from tryptophans. The single tryptophan mutants of the $G_{o\alpha}$ subunits provide new insights into structural determinants of nucleotide release and hydrolysis. They will also be useful tools in further examining G protein activation mechanisms with MANT-guanine nucleotide derivatives.

MATERIALS AND METHODS

Materials. Dithiothreitol (DTT) and guanosine 5′-*O*-(3-thiotriphosphate) (GTPγS) were purchased from CalBiochem (San Diego, CA). [^{3}H]GDP, [^{35}S]GTPγS, and [γ-^{32}P]GTP were obtained from New England Nuclear (Boston, MA). Trypsin was purchased from Sigma (St. Louis, MO). Ni^{2+}-NTA resin was from Qiagen (Chatsworth, CA). MANT-guanine nucleotide was synthesized and purified as described (*1*). The expression vectors pQE/$G_{o\alpha}$ and the hexahistidine-tagged pQE60/$G_{i\alpha}$ were generously provided by Dr. M. E. Linder (Washington University).

DNA Construction and Mutagenesis. In order to facilitate manipulations of the full-length $G_{o\alpha}$ coding sequence, the *Nco*I recognition site within the $G_{o\alpha}$ coding sequence was mutated by the megaprimer PCR mutagenesis technique (*20*). The mutagenic primer 5′-GCCATTGTGCGGGCTATG-GATACT-3′ was used with the flanking primer 5′-ACTC-CCGAGATCGGTTGAAGCACT-3′ to amplify a first round of PCR on the template plasmid pQE/$G_{o\alpha}$ and to introduce a silent mutation in the *Nco*I site. The PCR fragment was purified and used directly as a primer together with the other flanking primer, 5′-GAATTCATTAAAGAGGAGAAA-3′, to amplify a second round DNA synthesis using pQE/$G_{o\alpha}$ as template. The secondary PCR product was sequenced, digested with *Bst*XI and *Pst*I restriction enzymes, and ligated back into pQE/$G_{o\alpha}$. The full length of $G_{o\alpha}$ sequence in an *Nco*I/*Hin*dIII fragment was ligated into a *Nco*I/*Hin*dIII-digested pQE60/$G_{i\alpha}$ to yield the amino-terminal His_6 construct pQE60/$G_{o\alpha}$(*Nco*I$^-$). To introduce the tryptophan mutation in the $G_{o\alpha}$ sequence, a 419 bp *Pst*I and *Cla*I fragment was cut from the pQE/$G_{o\alpha}$ vector and ligated into the corresponding sites of pBluescript II SK. W132F, W212F, and W212A mutations were introduced by the same method using primers 5′-GAGTCGCCAAAGAGTCGCAT-CAT-3′, 5′-CTGAACGTAAGAAGTTTATCCACTGCTT-3′, and 5′-TGAACGTAAGAAGGCGATCCACTGCTTC-3′, respectively, and flanking primers, GTAAAACGACGGC-CAGTGAGC-3′ and 5′-CCTCACTAAAGGGAACAAAA-GC-3′, derived from pBluescript II SK. The *Pst*I/*Cla*I fragments with the introduced tryptophan mutations, W132F, W212F, or W212A, were cloned into corresponding sites of pQE60/$G_{o\alpha}$(*Nco*I$^-$). The sequence of all $G_{o\alpha}$ mutants was confirmed by dideoxy DNA sequencing over the PCR-amplified region.

Expression and Purification of His_6-Tagged $G_{o\alpha}$. $His_6G_{o\alpha}$ proteins were purified by a modification of the method of Lee et al. (*21*). The cDNAs of wild type or W132F, W212A, or W212F mutant hexahistidine-tagged $G_{o\alpha}$ in expression vector, pQE60, were transformed into the *E. coli* strain BL21/DE3. The cells were grown in 4 L of enriched medium (2% tryptone, 1% yeast extract, 0.5% NaCl, 0.2% glycerol, and 50 mM KH_2PO_4, pH 7.2) in the presence of 50 μg/mL ampicillin at 30 °C up to OD_{600} of 0.4 and then incubated for 18 h with IPTG (30 μM) and chloramphenicol (1 μg/mL). The bacterial cell pellet was frozen in liquid nitrogen, resuspended in $T_{50}\beta_{20}P_{0.1}$ (50 mM Tris-HCl, pH 8.0, 20 mM 2-mercaptoethanol, and 0.1 mM phenylmethanesulfonyl flouride), and incubated with 0.1 mg/mL lysozyme and 0.02 mg/mL DNase and 5 mM $MgSO_4$. The lysate was centrifuged at 4 °C for 30 min at 30 000 rpm (Beckman Ti 45 rotor). The supernatant was then applied to a 20-mL Ni^{2+}-NTA column (Qiagen) equilibrated with $T_{50}\beta_{20}P_{0.1}$ containing 100 mM NaCl. The column was washed with 80 mL of $T_{50}\beta_{20}P_{0.1}$ containing 500 mM NaCl and 10 mM imidazole. Proteins were eluted with $T_{50}\beta_{20}P_{0.1}$ containing 100 mM NaCl, 10% glycerol, and 100 mM imidazole. The protein in the peak fractions was further subjected to anion exchange chromatography on a Mono Q HR5/5 (Pharmacia Biotech) column using a BioCAD SPRINT System (Perspective Biosystems, Inc., Framingham, MA). The fractions of $His_6G_{o\alpha}$ proteins eluted in 25 mM Tris, 25 mM Bis Tris Propane, pH 8.0, and 20 mM NaCl buffer were concentrated by centricon-30 (Amicon, Inc., Beverly, MA), and stored at −80 °C for up to 6 months before use. GDP (1 μM) was added to purified proteins before freezing. The total amount of purified proteins was measured by Bradford assay (*22*), and the amounts of functional $His_6G_{o\alpha}$ proteins were determined by a GTPγS binding assay (*23*). The yield and specific activities of the purified proteins are shown in Table 1.

Determination of G Protein Concentration. For all experiments (binding, fluorescence, and GTPase), the amount of functional protein was determined by [^{35}S]GTPγS binding performed within 3 days of the experiment. In most cases, GTPγS binding was determined the same day as the functional experiment.

Fluorescence Measurements. Fluorescence measurements were determined using a PTI ALPHASCAN fluorometer (Photon Technology Intl., Monmouth Junction, NJ) with a water-cooled 150 W Xenon arc lamp as described (*1*). $His_6G_{o\alpha}$ proteins were diluted into buffer containing 50 mM

Hepes, pH 8.0, 1 mM EDTA, 1 mM DTT, 10 mM $MgSO_4$, and 20 ppm deionized Lubrol (HEDNML), placed in custom-made 5 mm round quartz cuvettes in temperature-controlled (20 °C) sample holders, and continuously stirred. Time course measurements of intrinsic fluorescence (λ_{ex} 280, λ_{em} 340 nm, 1 nm slits) were performed with 250 nM $His_6G_{o\alpha}$ proteins and 1 μM GTPγS in final volume of 0.2 mL. The fluorescence increase upon binding of mGTPγS to 25 nM $His_6G_{o\alpha}$ was detected by exciting $His_6G_{o\alpha}$ tryptophans at 280 nm and detecting MANT emission at 440 nm. The concentration of mGTPγS was saturating (2 μM). The time dependent fluorescence values were fit to a one-component exponential association curve using Prism (Graphpad Software, San Diego, CA).

Trypsin Proteolysis Assay. One microgram of $His_6G_{o\alpha}$ was preincubated with 100 μM GTPγS or 100 μM mGTPγS in HEDNML buffer for 20 min at 20 °C. Twenty nanograms of typsin was added and the incubation continued for 30 min. Trypsin-digested samples were analyzed by 11% SDS−PAGE and visualized by Coomassie Blue. The gels were scanned (Scan Jet IIC, Hewlett Packard), and the 37 kDa bands were quantitated (IMAGE QUANT, Molecular Dynamics).

Saturation of $His_6G_{o\alpha}$ by [^{3}H]GDP and Equilibrium Guanine Nucleotide Binding. Ten nanomolar $His_6G_{o\alpha}$ proteins was incubated with 10−2000 nM [^{3}H]GDP in HEDNML buffer in the presence or absence of 2 μM GTPγS (to determine the nonspecific binding). Following incubation at 20 °C for 1 h, the samples were filtered onto BA85 nitrocellulose filters (Schleicher & Schuell, Keene, NH), and the filters were washed with ice-cold 20 mM Tris, 100 mM NaCl, and 25 mM $MgCl_2$, pH 8.0. The filters were counted in 4 mL of ScintiVerse scintillation cocktail (Fisher Scientific, Fair Lawn, NJ). Equilibrium competition experiments were performed using [^{3}H]GDP and different unlabeled guanine nucleotide analogs to determine their binding constants for $His_6G_{o\alpha}$ as described (*1*). Twenty nanomolar $His_6G_{o\alpha}$ proteins was preincubated in HEDNML buffer with 1−20 000 nM competing ligand for 30 min on ice before a final concentration of 100 nM [^{3}H]GDP was added. Following incubation with [^{3}H]GDP for 1 h at 20 °C, the samples were filtered as in the saturation experiments. The data were fitted by nonlinear least-squares analysis with hyperbolic or competition binding functions using Graphpad Prism. IC_{50} values from competition experiments were converted to K_i's by the method of Cheng and Prusoff (*24*).

GTPase Activity. The GTPase activity of $His_6G_{o\alpha}$ proteins was measured as described with some modification (*7*). Five nanomolar $His_6G_{o\alpha}$ was incubated with concentrations of [γ-^{32}P]GTP (7500 cpm/pmol) ranging from 0.05 to 5 μM in HEDNML buffer at 20 °C. The assay was initiated by addition of [γ-^{32}P]GTP solution, and 50 μL aliquots were taken and diluted in 1 mL of 15% (w/v) charcoal solution (50 mM NaH_2PO_4, pH 2.3, 0 °C) at 5 min intervals for 30 min. Background hydrolysis was determined in the absence of protein and represents less than 10% of total [γ-^{32}P]P_i release.

Determination of k_{cat} for Hydrolysis of GTP. Ten nanomolar $His_6G_{o\alpha}$ was incubated at room temperature (20−24 °C) in magnesium-free HEDNL buffer with 1 μM [γ-^{32}P]-GTP (7500 cpm/pmol) for 20 min to allow the proteins to bind GTP. The reaction was then started by addition of $MgSO_4$ and GTPγS to final concentrations of 20 mM and 200 μM, respectively. $MgSO_4$ activates $His_6G_{o\alpha}$ and triggers catalysis, while GTPγS prevents [γ-^{32}P]GTP from rebinding to the G protein. The amount of [γ-^{32}P]P_i released at each time point was fit to an exponential function: $cpm(t) = cpm_o + \Delta cpm \times (1 - e^{-kt})$.

Data Analysis and Statistics. Graphpad Prism (Graphpad Software, San Diego, CA) was used for unweighted nonlinear least-squares fitting of all of the data. The results are expressed as mean ± SEM.

Table 1: Purification and Characterization of Mutant $His_6G_{o\alpha}$ Protein[a]

$His_6G_{o\alpha}$	yield/L of prepn (mg)	sp act. (pmol/μg)	K_d for GDP[b] (nM)	app K_i for mGTPγS[d] (nM)
WT	1.1 ± 0.2 (2)	8.3 ± 1.4 (3)	87 ± 21 (3)	18 ± 5 (4)
W132F	0.63 ± 0.24 (2)	13.6 ± 2.3 (3)	137 ± 32 (3)	8 ± 4 (4)
W212F	0.45 ± 0.07 (2)	11.5 ± 1.8 (3)	38 ± 9 (3)	11 ± 2 (4)
W212A	0.40 (1)	6.7 ± 1.1 (3)	ND[c]	ND[c]

[a] One or two preparations of wild-type $His_6G_{o\alpha}$ and each mutant were done as described under Materials and Methods. The yield, specific activity, and affinity for GDP were determined, and the mean ± SEM (or SD for $n = 2$) is shown. The theoretical specific activity of pure and 100% functional $His_6G_{o\alpha}$ is 25 pmol/μg. [b] Saturation binding curves for [^{3}H]GDP were done as described under Materials and Methods. There was no significant difference in the K_d for GDP between the mutants (W132F and W212F) and the WT protein ($P > 0.05$). [c] Not determined. [d] K_i values for mGTPγS binding were determined by competition with binding of 100 nM [^{3}H]GDP as described under Materials and Methods.

RESULTS

Expression and Nucleotide Binding of Tryptophan Mutants. The wild-type and mutant $His_6G_{o\alpha}$ proteins were expressed and purified as described under Materials and Methods. All three single tryptophan mutants (W132F, W212F, and W212A) expressed well and were active (Table 1); however, a double tryptophan mutant, W132F/W212F, could not be expressed in active form despite several attempts. The affinities of the $His_6G_{o\alpha}$ W132F and W212F for GDP were not significantly different from that of WT protein (Table 1, $p > 0.05$). mGTPγS bound with comparable K_i values to WT, W132F, and W212F as measured by competition with [^{3}H]GDP binding (Table 1). Similarly, the K_i's of mutant $His_6G_{o\alpha}$ for mGppNHp and GTPγS were not significantly different from wild type (data not shown).

Fluorescence Properties of Tryptophan Mutants. We studied the intrinsic (tryptophan) and extrinsic (MANT nucleotide) fluorescence of the WT and mutant $His_6G_{o\alpha}$ to understand the contributions of the two tryptophans to these signals. Intrinsic fluorescence changes of WT, W132F, and W212F were monitored after addition of 1 μM GTPγS (Figure 1A). The maximal fluorescence increase of W132F on binding GTPγS was the same as that of WT, whereas W212F failed to exhibit any fluorescence increase. These results show that W^{212} in $G_{o\alpha}$ [as with W^{207} in G_t (*9*)] is the only tryptophan with fluorescence emission sensitive to the conformational change of G_α upon activation. In order to determine whether resonance energy transfer from tryptophan contributed to the MANT guanine nucleotide fluorescence, the fluorescence changes on mGTPγS binding to the $G_{o\alpha}$ mutants were assessed. The kinetics of the fluorescence

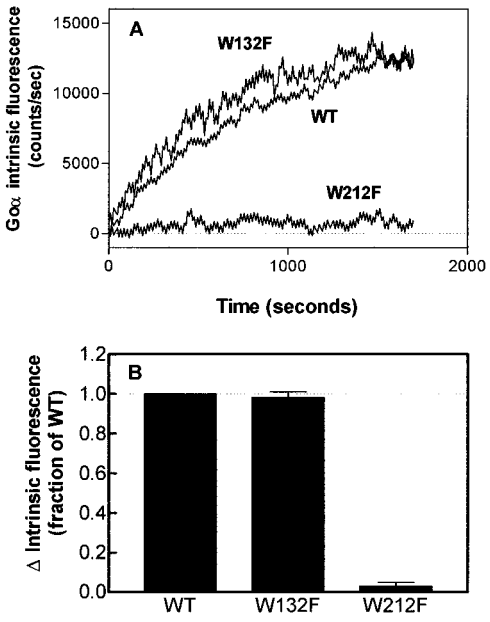

FIGURE 1: Intrinsic fluorescence changes in $His_6G_{o\alpha}$ upon binding GTPγS. (A) $His_6G_{o\alpha}$ proteins (250 nM) were preincubated 2 min at 20 °C in HEDNML buffer before addition of GTPγS (1 μM) at time zero. Fluorescence was monitored at 340 nm (λ_{ex}: 290 nm). The fluorescence of buffer and protein alone was subtracted. (B) The change in fluorescence upon addition of GTPγS was determined from a nonlinear least-squares fit of the time course data to a one component exponential association function. Values of the fitted ΔF are shown for three experiments with the mutants expressed as a fraction of the result with the wild-type protein. Data are presented as mean ± SEM for three experiments. The rate of the intrinsic fluorescence increase of $His_6G_{o\alpha}$ is slower than the rate of mGTPγS fluorescence change (Figure 2) and may be due to a higher concentration of GDP present in this experiment.

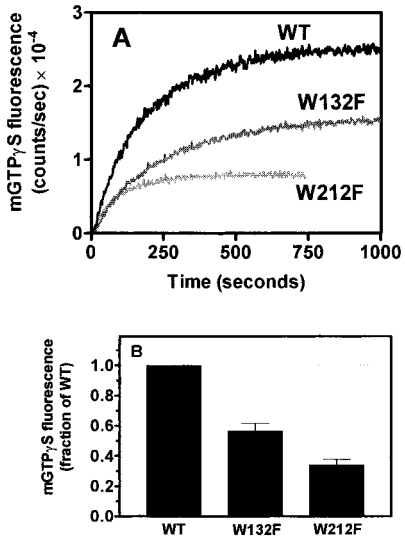

FIGURE 2: mGTPγS fluorescence change upon binding $His_6G_{o\alpha}$. (A) mGTPγS (2 μM) was added to 25 nM $His_6G_{o\alpha}$ (WT or mutant) in HEDNML buffer at 20 °C, and the fluorescence was monitored as described under Materials and Methods. Data were fit to a one component exponential association function, and the maximum fluorescence determined from the fit was determined. The rates of mGTPγS binding are listed in Table 3. Shown is a representative experiment that was repeated 6 times with similar results. (B) The maximal mGTPγS fluorescence increase when bound to W132F and W212F $His_6G_{o\alpha}$ proteins was calculated as a fraction of the value for WT $His_6G_{o\alpha}$. Data are presented as mean ± SEM for six experiments.

increase with excitation at 280 nm and emission at 440 nm are shown in Figure 2A. The fluorescence reached a plateau by 10−15 min, and higher concentrations of mGTPγS did not produce any further increase in fluorescence. The maximal fluorescence values of mGTPγS bound to W132F and W212F were 57 ± 6% and 34 ± 4%, respectively, of that with WT (Figure 2B). This does not appear to be due to decreased affinity of the mGTPγS as the amount used (2 μM) was substantially greater than the K_i for mGTPγS binding for all proteins (Table 1). After the mGTPγS fluorescence was at a maximum, emission and excitation spectra were obtained (Figure 3A,B). The mGTPγS emission peak at 440 nm was not significantly shifted but was much lower with W132F and W212F compared to WT. In the excitation spectrum, the peak at about 285 nm has been attributed to energy transfer from tryptophan while the 340 nm peak is due to direct excitation of the MANT moiety. The reduced excitation at 280 nm in the two mutants indicates that W^{132} and W^{212} both contribute significantly to the mGTPγS fluorescence, consistent with resonance energy transfer from W^{132} as well as W^{212}. This is in marked contrast to the intrinsic fluorescence change which is unaffected by removal of W^{132}.

Normal "Activation" of Mutant Proteins by Nucleotides. The decreased mGTPγS fluorescence signal with mutant proteins suggests that both tryptophan residues contribute to mGTPγS fluorescence; however, the lower fluorescence signal may be due to an altered activated conformational change compared to WT. To exclude this possibility, a

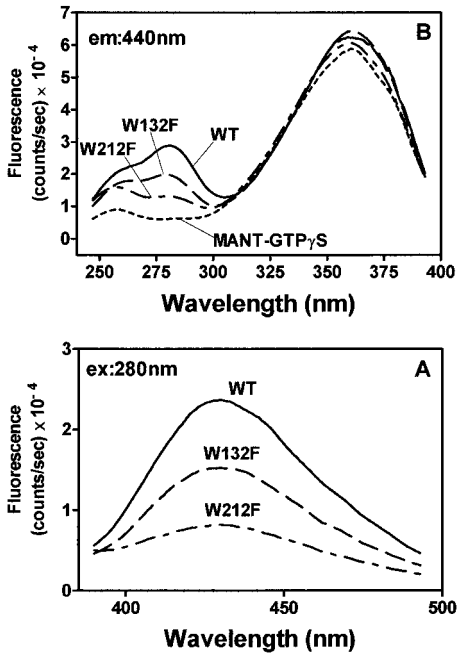

FIGURE 3: Emission and excitation spectra for mGTPγS bound to $His_6G_{o\alpha}$. (A) Emission spectra (280 nm excitation) of 25 nM WT (—), W132F (— —), and W212F (— - —) $His_6G_{o\alpha}$ with 2 M mGTPγS and 2 μM mGTPγS alone (---) were obtained after fluorescence had reached the maximum as shown in Figure 2. The spectrum obtained with HEDNML buffer alone has been subtracted in each case. (B) Excitation spectra (440 nM emission) were monitored as in emission spectra. The HEDNML buffer alone spectrum has been subtracted.

trypsin proteolysis protection experiment was performed. $His_6G_{o\alpha}$ proteins were incubated with 100 μM either GTPγS or mGTPγS at 20 °C for 20 min followed by trypsin addition. As previously described (*19*, *25*), the protected $His_6G_{o\alpha}$ was

Table 2: Trypsin Digestion of Guanine Nucleotide Activated $His_6G_{o\alpha}$ Proteins[a]

condition	density of 37 kDa band, % of control (*n*)		
	WT	W132F	W212F
no nucleotide + trypsin	4 ± 1 (3)	4 ± 1 (3)	8 ± 2 (3)
GTPγS (100 μM) + trypsin	71 ± 13 (5)	68 ± 14 (5)	78 ± 15 (4)
mGTPγS (100 μM) + trypsin	72 ± 14 (5)	62 ± 9 (5)	68 ± 19 (4)

[a] One microgram of $His_6G_{o\alpha}$ was preincubated with 100 μM either GTPγS, mGTPγS, or no nucleotide in HEDNML buffer for 20 min at 20 °C. Twenty nanograms of typsin was added and the incubation continued for 30 min. Control and trypsin-digested samples were analyzed by 11% SDS−PAGE and visualized by Coomassie Blue. The gels were scanned (Scan Jet IIC, Hewlett Packard), and the 37 kDa bands were quantitated (IMAGE QUANT, Molecular Dynamics). The amount of 37 kDa band remaining after reaction with trypsin was quantitated and normalized to the amount of 40 kDa band in the undigested sample. The results represent the mean ± SEM of the indicated times of experiments.

revealed as a 37 kDa band on a SDS 10% gel. This 37 kDa band was quantitated, and the results were normalized to the amount of undigested protein (Table 2). There were no significant differences in the amount of $His_6G_{o\alpha}$ protected by 100 μM of either GTPγS or mGTPγS. Thus, all proteins were equally activated by guanine nucleotides, and the lower maximal mGTPγS fluorescent signal for tryptophan mutants was not due to incomplete or altered G_α activation.

Kinetics of GDP Release from W132F and W212F Mutants. The rate constant for the mGTPγS fluorescence increase reflects the GDP release rate since GDP release is slow (*26*). At lower concentrations of mGTPγS (and in the GTPγS experiments in Figure 1), endogenous GDP competed with mGTPγS for $His_6G_{o\alpha}$, and the fluorescence increase was slower than expected based on literature values of the GDP release rate, $k_{off,GDP}$. In order to accurately estimate the $k_{off,GDP}$ (Figure 2), increased concentrations of mGTPγS were used, and the rate constant for mGTPγS fluorescence reached a plateau at mGTPγS concentrations greater than or equal to 2 μM. The rates of mGTPγS binding were 0.25 ± 0.03, 0.14 ± 0.02, and 0.54 ± 0.08 min^{-1}, for WT, W132F, and W212F, respectively. These data show that the perturbation caused by mutation of the tryptophan in the helical domain (W^{132}) slows GDP release, whereas modification of the GTPase domain (W^{212}) accelerates GDP release.

W^{212} Reduces k_{cat} for GTP Hydrolysis. To determine whether mutation from tryptophan to phenylalanine in the helical and GTPase domains changed the functional properties of the $His_6G_{o\alpha}$ protein other than the GDP release rate, we examined the steady-state GTPase activity. We expected the W212F mutant, which has a faster GDP release rate, to show an increased V_{max} for GTP hydrolysis while W132F would have a lower V_{max} than WT. WT and W132F demonstrated steady-state V_{max} values of 0.30 ± 0.03 and 0.13 ± 0.01 min^{-1}, respectively (Figure 4), which were compatible with the GDP release rate determined from mGTPγS fluorescence studies (Table 3). However, W212F actually showed a lower steady-state GTP hydrolysis rate in contrast to the increase expected from its faster mGTPγS binding. This suggests that for W212F, the steady-state GTP hydrolysis rate may be limited by k_{cat} instead of $k_{off,GDP}$. To test this possibility, k_{cat} values for each of the $His_6G_{o\alpha}$ proteins were estimated by single turnover experiments (Figure 5) as described [Berman et al., 1996 (*7*); Materials and Methods]. GTP hydrolysis by W212F was reduced compared to that for WT and W132F proteins as predicted. The observed rates were 1.39 ± 0.19, 1.0 ± 0.16, and 0.52 ± 0.06 min^{-1} for WT, W132F, and W212F, respectively (Figure 5 and Table 3). To confirm that the kinetic changes were due to removal of the W^{212} and not substitution of the phenylalanine, we prepared a W212A mutant and tested its catalytic properties. It also showed a much reduced k_{cat} (Table 3); however, it was not quite slow enough to fully account for the low steady-state V_{max} value (see Discussion).

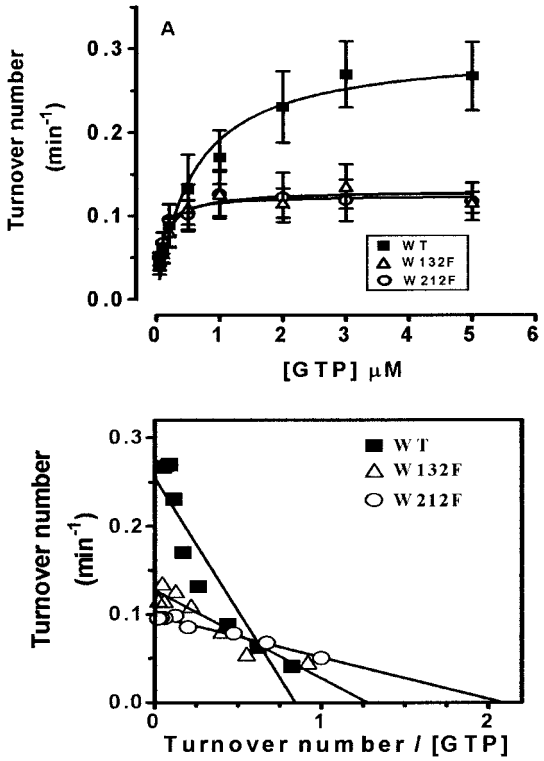

FIGURE 4: Steady-state GTPase activities of WT and mutant $His_6G_{o\alpha}$. (A) Steady-state GTPase activities were measured with 5 nM $His_6G_{o\alpha}$ proteins (WT, filled squares; W132F, open triangles; W212F, open circles) incubated with the indicated concentrations of GTP as described under Materials and Methods. The base line value representing less than 10% of total [γ-^{32}P]P_i release was determined in the absence of protein and was subtracted. The data were fit to the function $V = V_{max}S/(S + K_m)$ to determine the kinetic parameters. Shown are means ± SEM of the data from five experiments. The average K_m values for WT, W132F, and W212F $His_6G_{o\alpha}$ are 570 ± 220, 110 ± 50, and 80 ± 30 nM, respectively (n = 5), and the V_{max} values are 0.30 ± 0.03, 0.13 ± 0.01, and 0.12 ± 0.01 min^{-1}, respectively. (B) An Eadie−Hofstee plot is shown of the data in (A). The y-intercept indicates V_{max}, and the slope is $-K_m$. The symbols are the same as in (A).

DISCUSSION

In this report, we describe the expression and characterization of single tryptophan mutants of the $G_{o\alpha}$ protein. These data confirm results observed with the transducin α subunit in that the α2 helix tryptophan (W^{212} in $G_{o\alpha}$ and W^{207} in transducin) is the only tryptophan contributing to the intrinsic fluorescence change upon protein activation (*9*). They also validate our previous hypothesis (*1*, *19*) that the fluorescence signal detected for heterotrimeric G proteins binding MANT guanine nucleotides involves energy transfer from tryptophan but interestingly both tryptophans are involved. Finally, significant functional changes are seen with mutations in each

Table 3: Kinetic Parameters of Nucleotide Binding and GTP Hydrolysis by $His_6G_{o\alpha}$ Proteins

kinetic parameters	WT	W132F[b]	W212F[b]	W212A
V_{max} (min^{-1})[a]	0.30 ± 0.03 (5)	0.13 ± 0.01* (5)	0.12 ± 0.01* (5)	ND[f]
K_m (nM)[a]	570 ± 220 (5)	110 ± 50* (5)	80 ± 30* (5)	ND[f]
$k_{off,GDP}$ (min^{-1})[c]	0.25 ± 0.03 (6)	0.14 ± 0.02 (6)	0.54 ± 0.08 (6)	ND[f]
$k_{on,GDP}$ (min^{-1} nM^{-1})[d]	0.0029 ± 0.0010 (3)	0.0010 ± 0.0003 (3)	0.014 ± 0.003 (3)	ND[f]
k_{cat} (min^{-1})[e]	1.39 ± 0.19 (9)	1.0 ± 0.16 (4)	0.52 ± 0.06 (9)	0.26 ± 0.10 (3)

[a] $His_6G_{o\alpha}$ proteins were incubated with different concentrations of GTP, and steady-state GTP hydrolysis rates were obtained and fitted by nonlinear least-squares regression to hyperbolic curves as described in the legend to Figure 4. Values shown are mean ± SEM of 5 replicate experiments. This table shows the turnover number (V_{max}) determined from data in Figure 4A and similar experiments compared to the rate constant for the fluorescence increase upon binding of 2 μM mGTPγS (Figure 2A). GDP release kinetics are likely the rate-limiting step for the mGTPγS binding experiments. [b] A *t*-test was performed to compare the V_{max} and K_m values of mutant $His_6G_{o\alpha}$ proteins with those of wild type. * indicates $P < 0.01$. [c] $k_{on,mGTP\gamma S}$ is used to represent $k_{off,GDP}$. [d] $k_{on,GDP}$ (min^{-1} nM^{-1}) is calculated from $k_{off,GDP}$ (min^{-1})/K_d (nM). The standard deviation of each data point has been considered in individual calculation. [e] k_{cat} (min^{-1}) of WT recombinant $G_{o\alpha}$ from other literature was 2.2 ± 0.3 min^{-1} (*34*).[f] Not determined.

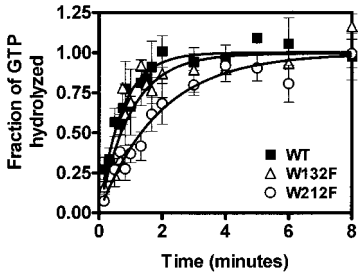

FIGURE 5: Determination of k_{cat}. $His_6G_{o\alpha}$ proteins (10 nM) were incubated at room temperature (23−24 °C) in magnesium-free buffer (HEDNL) with 1 μM [γ-^{32}P]GTP (7500 cpm/pmol) for 20 min. The reaction was started at time zero as indicated by addition of $MgSO_4$ and GTPγS to final concentrations of 20 mM and 200 μM, respectively. Base line [γ-^{32}P]GTP hydrolysis was measured at 5, 10, and 15 min before the beginning of the reaction, and the value predicted for time zero was subtracted from the data. GTP hydrolysis at indicated time points was calculated as a fraction of the total GTP hydrolyzed The data were fitted to a single exponential association function (Graphpad Prism), and the results are listed in Table 3.

tryptophan. Mutation of W^{132} to phenylalanine only alters GDP release resulting in a 2-fold slowing. In contrast, mutation of W^{212} increases the GDP release rate but also causes a 3−5-fold reduction in k_{cat}.

Conservation of the G Protein Activation Sensor. In examining the tryptophan mutants of $G_{o\alpha}$, one of the most striking observations was that the intrinsic fluorescence signal was totally lost for the W212F mutant and completely normal for the W132F mutant. Chabre and colleagues (*9*) showed similar results for W^{207} in transducin but did not test the effect of modifying W^{127}. Our data confirm their conclusions and extend them to $G_{o\alpha}$. The available crystal structures now provide a clear explanation of these results. Tryptophan 211 in G_i shows considerably more solvent exposure in the heterotrimer (GDP-bound) than in the activated (GTPγS-bound) state while W^{132} shows virtually no change in environment upon subunit activation (*17*, *27*). Faurobet et al. (*9*) also found that the W^{207} mutation prevented cGMP phosphodiesterase activation. Unfortunately, there is no simple test for $G_{o\alpha}$ effector function as many of the effects of $G_{o\alpha}$ are due to release of the $\beta\gamma$ subunit rather than to the activated $G_{o\alpha}$ itself (*5*, *4*). However, we can say that the W212F mutant does undergo the conformational change generally associated with activation as the protection of K^{210} from digestion by trypsin does occur.

Energy Transfer from Tryptophans to MANT-Guanine Nucleotides. We have described, in previous work, substantial evidence that the fluorescence signal from MANT-containing guanine nucleotides is related to the activation of heterotrimeric G protein α subunits (*1*, *19*). Indeed, there were smaller fluorescence signals from mGppNHp and $mGppCH_2p$ which correlated with partial activation of the Gα subunits by those nucleotides. The structural and mechanistic basis for the conformation-dependent fluorescence remains unclear. The data presented here confirm the role of tryptophan energy transfer in the MANT-nucleotide fluorescence and provide important tools (i.e., single tryptophan mutants) to further examine conformational changes associated with G protein activation. The distances between W^{132} and W^{212} and the guanine nucleotide are nearly optimal for detecting small changes in G protein structure. In the crystal structure of $G_{i\alpha1}$, the distances between W^{212} and the ribose O2 position on GTPγS (*17*, *27*) are 17.4 and 20.6 Å, respectively. For W^{132}, the distances are 14.4 and 13.0 Å, respectively. Estimates of the R_0 for energy transfer from tryptophan to MANT range from 12 to 22 Å.[2] In addition to the distance changes, there is a very substantial rotation of W^{212} upon $G_{o\alpha}$ activation which may cause significant orientational effects as well. While orientational effects are not common in protein fluorescence, in this case both the tryptophan and the MANT moiety are likely to be in fairly constrained positions. More detailed fluorescence studies, including tryptophan lifetimes, are currently in progress.

Structural Determinants of GDP Release Rates. In addition to the spectroscopic changes, the tryptophan mutations resulted in functional alterations in $G_{o\alpha}$ as well. The rate of GDP release was affected in opposite directions by the two tryptophan mutations. Mutations which enhance GDP release rates are fairly common and have been frequently identified in the carboxyl terminus of the α subunit (*28*, *29*, *17*). In the case of W^{212}, the mutation is close to the nucleotide binding site, and it is easy to see how perturbation of the binding pocket might enhance the rate of GDP release. Despite the larger value of $k_{off,GDP}$, the K_d for GDP is actually lower, giving a faster $k_{on,GDP}$ as well. Thus, it is important to keep in mind that a faster dissociation rate constant does not automatically translate to a lower affinity. It is likely that the W^{212} mutation results in a more

[2] The R_0 calculations for tryptophan to MANT energy transfer used the following assumptions: quantum yield of tryptophan, 0.14; orientation factor (κ^2) of 0.67; dielectric constant for the interior of Gα subunit ranging from 2 to 5. The extinction coefficient used for mantGTPγS was 22 500 cm^{-1} M^{-1} as previously reported (*1*). Modest changes in any of these parameters do not strongly affect the range of R_0 values.

"open" binding pocket. In contrast, the W132F mutation results in slower rates than WT for both GDP dissociation and association. Again the association rate is affected more, so the K_d changes in the opposite direction from that expected from the decreased $k_{off,GDP}$. The reduction in the GDP release rate is modest but does implicate the helical domain of the G α subunit as a potential regulator of GDP release. The R178C mutation in $G_{i\alpha}$ which markedly reduces k_{cat} also reduces $k_{off,GDP}$ by approximately 2-fold (*30*). This arginine is in the junction between the helical and GTPase domains. The effect of these two mutants, W132F in $G_{o\alpha}$ and R178C in $G_{i\alpha}$, suggests that collapse of the helical domain onto the GTPase domain may "tighten" the nucleotide binding site and reduce GDP release rates. Similarly, transducin may have a restricted binding pocket as it has a very slow basal GDP release rate and MANT nucleotides bind with low affinities (*31*).

Effect of W^{212} Mutations on GTP Hydrolysis. Numerous mutations of G_α subunits reduce GTP hydrolysis. In $G_{i\alpha}$, R187C, Q204L, and S47N all reduce the k_{cat} for GTP hydrolysis (*32*, *33*). We now add W212F and W212A to this list, though their effects are not as striking (3−5-fold reduction) as the other mutations. For both WT and W132F, the steady-state V_{max} for GTPase is identical to the rate of GDP release as expected. In contrast, for the W212F mutant, the steady-state V_{max} is lower than both the GDP release rate and the k_{cat} determined experimentally. We cannot fully explain this discrepancy though it could be due to experimental error, different temperatures of the two experiments (20 °C vs 24 °C), or a different rate limiting step (e.g., phosphate release).

In summary, the spectroscopic and functional properties of single tryptophan mutants of $G_{o\alpha}$ provide new information about the source of spectroscopic signals and a role for tryptophan 212 in structural determinants of nucleotide binding and hydrolysis.

ACKNOWLEDGMENT

We thank Dr. M. E. Linder (Washington University) for generously providing the pQE/$G_{o\alpha}$ and the his_6-tagged expression vector pQE60/$G_{i\alpha}$.

REFERENCES

1. Remmers, A. E., Posner, R., and Neubig, R. R. (1994) *J. Biol. Chem. 269*, 13771−13778.
2. Freissmuth, M., Casey, P. J., and Gilman, A. G. (1989) *FASEB J. 3*, 2125−2131.
3. Clapham, D. E., and Neer, E. J. (1993) *Nature 365*, 403−406.
4. Herlitze, S., Garcia, D. E., Mackie, K., Hille, B., Scheuer, T., and Catterall, W. A. (1996) *Nature 380*, 258−262.
5. Ikeda, S. R. (1996) *Nature 380*, 255−258.
6. Dohlman, H. G., Apaniesk, D., Chen, Y., Song, J., and Nusskern, D. (1995) *Mol. Cell Biol. 15*, 3635−3643.
7. Berman, D. M., Wilkie, T. M., and Gilman, A. G. (1996) *Cell 86*, 445−452.
8. Berstein, G., Blank, J. L., Jhon, D. Y., Exton, J. H., Rhee, S. G., and Ross, E. M. (1992) *Cell 70*, 411−418.
9. Faurobert, E., Otto-Bruc, A., Chardin, P., and Chabre, M. (1993) *EMBO J. 12*, 4191−4198.
10. Mittal, R., Cerione, R. A., and Erickson, J. W. (1994) *Biochemistry 33*, 10178−10184.
11. Phillips, W. J., and Cerione, R. A. (1988) *J Biol. Chem. 263*, 15498−15505.
12. Guy, P. M., Koland, J. G., and Cerione, R. A. (1990) *Biochemistry 29*, 6954−6964.
13. Higashijima, T., Ferguson, K. M., Sternweis, P. C., Ross, E. M., Smigel, M. D., and Gilman, A. G. (1987) *J. Biol. Chem. 262*, 752−756.
14. Higashijima, T., Ferguson, K. M., Smigel, M. D., and Gilman, A. G. (1987) *J. Biol. Chem. 262*, 757−761.
15. Lambright, D. G., Noel, J. P., Hamm, H. E., and Sigler, P. B. (1994) *Nature 369*, 621−628.
16. Noel, J. P., Hamm, H. E., and Sigler, P. B. (1993) *Nature 366*, 654−663.
17. Coleman, D. E., Berghuis, A. M., Lee, E., Linder, M. E., Gilman, A. G., and Sprang, S. R. (1994) *Science 265*, 1405−1412.
18. Mixon, M. B., Lee, E., Coleman, D. E., Berghuis, A. M., Gilman, A. G., and Sprang, S. R. (1995) *Science 270*, 954−960.
19. Remmers, A. E., and Neubig, R. R. (1996) *J. Biol. Chem. 271*, 4791−4797.
20. Chen, B., and Przybyla, A. E. (1994) *BioTechniquies 17*, 657−659.
21. Lee, E., Linder, M. E., and Gilman, A. G. (1994) *Methods Enzymol. 237*, 146−163.
22. Bradford, M. M. (1976) *Anal. Biochem. 72*, 248−254.
23. Northup, J. K., Smigel, M. D., and Gilman, A. G. (1982) *J. Biol. Chem. 257*, 11416−11423.
24. Cheng, Y., and Prusoff, W. H. (1973) *Biochem. Pharmacol. 22*, 3099−3108.
25. Hurley, J. B., Simon, M. I., Teplow, D. B., Robishaw, J. D., and Gilman, A. G. (1984) *Science 226*, 860−862.
26. Ferguson, K. M., Higashijima, T., Smigel, M. D., and Gilman, A. G. (1986) *J. Biol. Chem. 261*, 7393−7399.
27. Wall, M. A., Coleman, D. E., Lee, E., Iniguez-Lluhi, J. A., Posner, B. A., Gilman, A. G., and Sprang, S. R. (1995) *Cell 83*, 1047−1058.
28. Skiba, N. P., Bae, H., and Hamm, H. E. (1996) *J. Biol. Chem. 271*, 413−424.
29. Denker, B. M., Schmidt, C. J., and Neer, E. J. (1992) *J. Biol. Chem. 267*, 9998−10002.
30. Kleuss, C., Raw, A. S., Lee, E., Sprang, S. R., and Gilman, A. G. (1994) *Proc. Natl. Acad. Sci. U.S.A. 91*, 9828−9831.
31. Zera, E. M., Molloy, D. P., Angleson, J. K., Lamture, J. B., Wensel, T. G., and Malinski, J. A. (1996) *J. Biol. Chem. 271*, 12925−12931.
32. Graziano, M. P., Freissmuth, M., and Gilman, A. G. (1989) *J Biol. Chem. 264*, 409−418.
33. Slepak, V. Z., Wilkie, T. M., and Simon, M. I. (1993) *J. Biol. Chem. 268*, 1414−1423.
34. Linder, M. E., Ewald, D. A., Miller, R. J., and Gilman, A. G. (1990) *J. Biol. Chem. 264*, 8243.

BI972122I